Atomic Masses in the Region Xenon to Europium*

W. H. JOHNSON, JR., AND A. O. NIER
Department of Physics, University of Minnesota, Minneapolis, Minnesota
(Received October 25, 1956)

A six-inch double-focusing mass spectrometer employing the peak matching method of measurement has been used to measure 36 atomic masses in the region $130 \leqq A \leqq 154$ and $54 \leqq Z \leqq 63$. Atomic masses of 41 radioactive nuclei have then been calculated from mass differences derived from nuclear reaction and β-decay energies. Nucleon binding and pairing energies have been calculated from the resulting mass table. The effect of the shell closure at $N=82$ on the systematics of nuclear binding and pairing energies has been investigated in greater detail than has previously been possible. The discontinuity in neutron binding energy, observed in reaction measurements and β-decay systematics, is shown to be caused by a decrease in binding energy of neutrons beyond $N=82$ rather than a particular large binding energy at $N=82$. The systematic behavior of proton binding and pairing energies is also studied. The nucleon binding and pairing energy results show departures from uniformity in the region near $N=90$. Electric quadrupole systematics have also indicated a change in nuclear structure in this region. The present atomic masses are also employed in the isotopic identification of several reactions, in the study of several natural alpha decays, and in the interpretation of several β-decay disintegration schemes.

INTRODUCTION

THIS paper presents the results of a portion of the program of mass measurement undertaken with double-focusing mass spectrometers developed at the University of Minnesota. Determinations of stable atomic masses in the region about the 20, 28, and 50 proton and neutron shells have been reported.[1–5] The atomic mass measurements reported here deal with the mass region about the 82 neutron shell closure. Determinations of 36 atomic masses in the region $A=130$ to 154 and $Z=54$ to 63 have been made by the doublet method, employing hydrocarbon comparison ions. By combining nuclear reaction Q-values and total β-decay energies with the stable masses, the atomic masses of 41 radioactive nuclei may be calculated. With these data it is possible to make a thorough study of the systematics of binding energies for nuclei in the neighborhood of the 82 neutron shell closure.

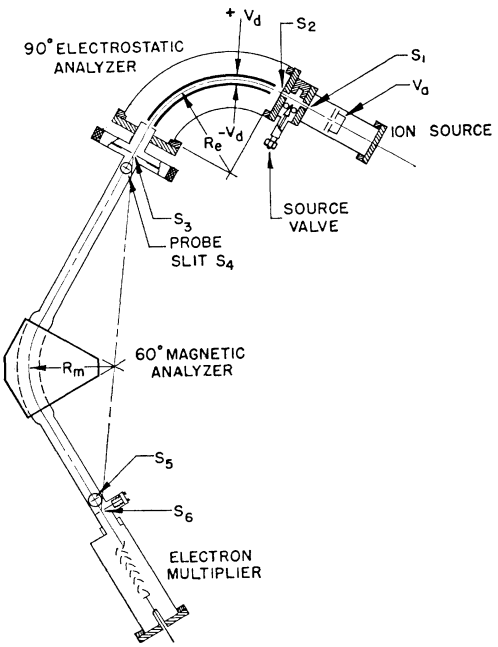

FIG. 1. A schematic diagram of the double-focusing mass spectrometer. R_e is 7.427 in. and R_m is 6.000 in. The accelerating voltage V_a is about 7600 v and the deflection plate voltage V_d is about 400 v. Typical slit dimensions are $S_1=S_6=0.0005$ in., $S_2=0.020$ in., and $S_3=0.010$ in. Slits S_4 and S_5 are employed to adjust the ion beam so that it lies in the dispersion plane. Ions are formed by electron impact. Metals to be run are placed in an electrically heated furnace in the source and vaporized. The detection system beyond the collector slit S_6 is a 10-stage silver-magnesium electron multiplier. An all-metal high vacuum source valve allows one to maintain a vacuum in the spectrometer tube while a change of sources is being made.

* This research is supported by a joint program of the Office of Naval Research and the U. S. Atomic Energy Commission.

APPARATUS

A 6-inch double-focusing mass spectrometer, constructed according to the design of Johnson and Nier,[6] was employed in this investigation. The combination of electrostatic and magnetic fields, shown schematically in Fig. 1, provides first- and second-order angle focusing and first-order energy focusing. This spectrometer has been described,[7] and has been used to determine a number of atomic masses.[1–4] However, instead of the original strip chart recording of data, the new null, peak-matching method of measurement is now employed.[8,9]

DOUBLET MASS DIFFERENCES

Table I lists the mass doublets measured and the mass differences obtained. The final doublet mass difference is the unweighted average of the individual

[1] Collins, Nier, and Johnson, Phys. Rev. **84**, 717 (1951).
[2] Collins, Nier, and Johnson, Phys. Rev. **86**, 408 (1952).
[3] Collins, Johnson, and Nier, Phys. Rev. **94**, 398 (1954).
[4] R. E. Halsted, Phys. Rev. **88**, 666 (1952).
[5] Quisenberry, Scolman, and Nier, Phys. Rev. **104**, 461 (1956).
[6] E. G. Johnson and A. O. Nier, Phys. Rev. **91**, 10 (1953).
[7] National Bureau of Standards Circular 522, 1953 (unpublished).
[8] C. F. Giese and T. L. Collins, Phys. Rev. **96**, 823(A) (1954).
[9] Quisenberry, Scolman, and Nier, Phys. Rev. **102**, 1071 (1956).

TABLE I. Mass doublets.

Doublet[a]	Mass difference[b] mMU
$C_6H_{10}O_3-Xe^{130}$	159.53 ±0.03
$C_6H_{10}O_3-Ba^{130}$	156.24 ±0.20
$C_{10}H_{11}-Xe^{131}$	181.05 ±0.04
$C_{10}H_{12}-Xe^{132}$	189.79 ±0.05
$C_{10}H_{12}-Ba^{132}$	188.84 ±0.12
$C_{10}H_{13}-Cs^{133}$	196.66 ±0.07
$C_{10}H_{14}-Xe^{134}$	204.20 ±0.05
$C_{10}H_{14}-Ba^{134}$	205.36 ±0.08
$C^{13}C_9H_{14}-Ba^{135}$	207.40 ±0.10
$C_{10}H_{16}-Xe^{136}$	218.055±0.025
$C_{10}H_{16}-Ba^{136}$	220.89 ±0.09
$C_{10}H_{16}-Ce^{136}$	218.19 ±0.20
$C^{13}C_9H_{16}-Ba^{137}$	223.08 ±0.06
$C_{10}H_{18}-Ba^{138}$	236.03 ±0.08
$C_{10}H_{18}-La^{138}$	234.17 ±0.20
$C_{10}H_{18}-Ce^{138}$	234.89 ±0.20
$C^{13}C_9H_{18}-La^{139}$	238.23 ±0.06
$C_{10}H_{20}-Ce^{140}$	251.29 ±0.06
$C_{11}H_9-Pr^{141}$	163.00 ±0.03
$C_{10}H_{22}-Ce^{142}$	262.93 ±0.07
$C_{10}H_{22}-Nd^{142}$	264.74 ±0.03
$C^{13}C_{10}H_{10}-Nd^{143}$	172.08 ±0.10
$C_{10}H_5F-Nd^{144}$	127.77 ±0.07
$C_{10}H_5F-Sm^{144}$	125.92 ±0.09
$C_{10}H_6F-Nd^{145}$	133.33 ±0.19
$C_{10}H_7F-Nd^{146}$	140.53 ±0.06
$C^{13}C_9H_7F-Sm^{147}$	142.09 ±0.03
$C_2{}^{13}C_8H_7F-Nd^{148}$	143.46 ±0.06
$C_9H_{10}O_2-Nd^{150}$	147.30 ±0.07
$C_9H_{10}O_2-Sm^{150}$	151.23 ±0.07
$C_{12}H_7-Eu^{151}$	135.26 ±0.17
$C_{13}H_{11}-Eu^{151}O^{16}$	171.69 ±0.19
$C_{12}H_8-Sm^{152}$	143.29 ±0.13
$C^{13}C_{12}H_{12}-Eu^{153}O^{16}$	181.8 ±0.4
$C_{12}H_{10}-Sm^{154}$	156.37 ±0.15

[a] Throughout this paper C, H, O, and F refer to C^{12}, H^1, O^{16}, and F^{19}, respectively.
[b] All calculations in this paper have been carried out with more significant figures than are indicated by the magnitude of the error. Results listed in all tables have been rounded off to conform with the size of the error.

runs. Five runs were recorded for most doublets. Each run is composed of 20 separate superpositions of the doublet constituents. No more than two runs on a particular doublet were made during any one day.

For these measurements, the width at half-height of a typical ion peak corresponded to a $\Delta m/m$ of about one part in 14 000. In the mass range investigated this resolution is insufficient to completely resolve the C^{13} satellite which contaminates to some extent most hydrocarbon ion peaks. For example, the hydrocarbon fragment C_mH_n is contaminated by the satellite $C^{13}C_{m-1}H_{n-1}$. A procedure was devised to correct each doublet measurement for this unresolved satellite. The possibility of an error in this correction is sufficiently great so that it seemed proper to consider that the error in the correction be equal to the correction itself. The final error in the doublet measurement is the square root of the sum of the squares of the C^{13} correction error and the statistical standard error associated with the set of individual runs that yield the final result. Because of the addition of the essentially nonstatistical satellite error, the statistical limit of error on a typical doublet is somewhat less than the usual factor of about three times the standard error. Errors arising from resistance calibration and leakage currents are small compared to the other errors and have been neglected.

MASSES

The atomic masses derived from the doublet data are listed in Table II. The typical accuracy of a stable mass value is about one part in two million; that is, approximately 0.075 mMU in this region. Secondary

TABLE II. Atomic masses computed from doublet data in Table I together with a comparison with previous mass spectroscopic values.

Isotope	Present result[a] (amu)	Previous result[a] (amu)
Xe^{130}	129.944 81 ±3	129.944 75 ±8[b]
Ba^{130}	129.948 10 ±20	
Xe^{131}	130.946 70 ±4	130.946 7 ±4[b]
Xe^{132}	131.946 11 ±5	131.946 68 ±30[c]
		131.946 05 ±15[b]
		131.945 90 ±12[b]
		131.946 115±9[d]
Cs^{133}	132.947 38 ±7	
Xe^{134}	133.947 99 ±5	133.947 75 ±10[b]
Ba^{134}	133.946 83 ±8	
Ba^{135}	134.948 45 ±10	
Xe^{136}	135.950 419±25	135.950 17 ±8[b]
Ba^{136}	135.947 58 ±9	
Ce^{136}	135.950 28 ±20	
Ba^{137}	136.949 06 ±6	
Ba^{138}	137.948 73 ±8	137.948 4 ±4[e,f]
La^{138}	137.950 59 ±20	
Ce^{138}	137.949 87 ±20	
La^{139}	138.950 20 ±6	
Ce^{140}	139.949 76 ±6	139.949 2 ±6[g,f]
Pr^{141}	140.952 28 ±3	140.951 3 ±3[h,i]
		140.950 9 ±3[e,i]
Ce^{142}	141.954 41 ±7	
Nd^{142}	141.952 60 ±3	
Nd^{143}	142.955 02 ±10	
Nd^{144}	143.955 56 ±7	143.955 9 ±4[g,i]
		143.955 22 ±20[g,f]
Sm^{144}	143.957 41 ±9	143.955 7 ±8[e,f]
Nd^{145}	144.958 14 ±19	
Nd^{146}	145.959 08 ±6	145.958 9 ±4[e,f]
Sm^{147}	146.961 20 ±3	
Nd^{148}	147.963 49 ±6	147.963 80 ±25[e,f](Ge[74])
		147.964 4 ±4[e,f](Se[74])
Sm^{148}	147.961 45 ±20[j]	147.960 9 ±4[e,f](Ge[74])
		147.962 1 ±6[e,f](Se[74])
Sm^{149}	148.964 15 ±20[j]	
Nd^{150}	149.968 49 ±7	149.967 2 ±5[g,i](Ti[50])
		149.968 2 ±4[g,f](As[75])
		149.968 5 ±4[e,f]
Sm^{150}	149.964 57 ±7	149.963 5 ±8[e,f]
Eu^{151}	150.967 55 ±17[k]	
	150.967 51 ±19[l]	
final	150.967 53 ±13	
Sm^{152}	151.967 67 ±13	151.967 04 ±25[e,f](Ge[76])
		151.968 2 ±6[e,f](Se[76])
Eu^{153}	152.969 2 ±4	
Sm^{154}	153.970 87 ±15	153.970 7 ±3[e,f]

[a] Throughout this paper, when masses are given in amu, the errors refer to the last significant figure of the particular result.
[b] R. E. Halsted, Phys. Rev. **88**, 666 (1952).
[c] C. L. Kegley and H. E. Duckworth, Nature **167**, 1025 (1951).
[d] K. S. Quisenberry (private communication).
[e] B. G. Hogg and H. E. Duckworth, Can. J. Phys. **32**, 65 (1954).
[f] Collins, Johnson, and Nier, Phys. Rev. **94**, 398 (1954).
[g] B. G. Hogg and H. E. Duckworth, Can. J. Phys. **31**, 942 (1953).
[h] Duckworth, Kegley, Olson, and Stanford, Phys. Rev. **83**, 1114 (1951).
[i] Collins, Nier, and Johnson, Phys. Rev. **86**, 408 (1952).
[j] Masses derived from isotopic mass unit data. See Table V.
[k] Derived from the $C_{12}H_7-Eu^{151}$ doublet.
[l] Derived from the $C_{13}H_{11}-Eu^{151}O$ doublet.

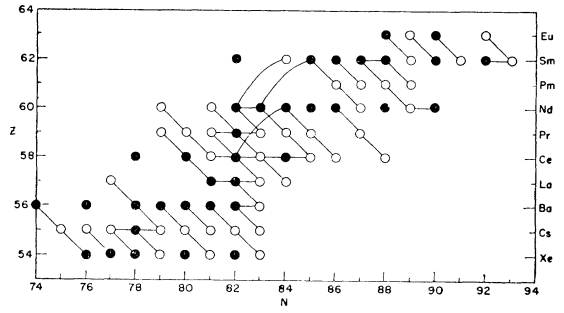

FIG. 2. Nuclear reaction and β-decay paths that were employed to calculate radioactive atomic masses. Solid circles indicate isotopes whose masses were determined in the present investigation. Open circles indicate the radioactive isotopes for which masses can be calculated. Connecting lines indicate available reaction and β-decay data.

standard masses employed in these calculations are $H^1 = 1.0081442 \pm 2$,[9] $C^{12} = 12.0038167 \pm 8$,[9] $C^{13} = 13.0074837 \pm 9$,[10] and $F^{19} = 19.0044429 \pm 20$ amu.[10] Included in Table II are previously obtained mass spectroscopic values.

Table III contains the atomic masses of 41 radioactive nuclei derived from stable atomic masses given in Table II together with mass differences from nuclear reaction Q values and β-decay energies. Figure 2 indicates the paths employed to calculate these mass differences. The majority of the reaction and β-decay data were obtained from review articles by Van Patter and Whaling,[11] and King.[12] Table IV lists new and revised data not included in these review articles. The mass-energy conversion factor, 1 amu = 931.141±0.010 Mev,[13] was employed. In several instances, the atomic mass of a particular radioactive nucleus is determined in more than one way. Generally, the several masses calculated for a given nucleus are in agreement. When the multiply determined masses were in agreement, a weighted average was used to obtain the final result. For Pr^{143} and Ce^{143}, where there was disagreement, an unweighted average was taken.

To verify the accuracy of the stable masses, a number of consistency tests have been applied to the data. The correctness of the spectrometer calibration can be verified by measuring hydrocarbon ion doublets having a mass difference of one hydrogen mass. Also, doublets that yield the $C^{13} - C^{12}$ mass difference can be measured. Six measurements of the former doublet yielded 1.00815±10 amu and five measurements of the latter yielded 1.00373±10 amu. These values are in good agreement with the accepted values of 1.0081442±2 and 1.0036670±12 amu, respectively.

For elements where it was possible, the mass difference between two isotopes differing by one mass number was directly measured. Such measurements test not only the instrument calibration but also the consistency of the doublet data. These results, called "isotopic

TABLE III. Atomic masses of radioactive nuclei which can be calculated from stable atomic masses using available mass differences from nuclear reaction data and β-decay energies.

Isotope	Atomic mass amu	Isotope	Atomic mass amu
Cs^{130}	129.948 02±4[a]	Nd^{141}	140.954 08±11
Cs^{131}	130.947 07±4	Pr^{142}	141.954 95±3[b]
Cs^{132}	131.948 10±20[b]	Ce^{143}	142.957 72±14[d]
Xe^{133}	132.947 84±7	Pr^{143}	142.956 20±14[d]
Cs^{134}	133.949 06±7[b]	Ce^{144}	143.959 08±7
La^{134}	133.950 83±25	Pr^{144}	143.958 75±7
Xe^{135}	134.949 93±10	Ce^{146}	145.964 68±14[c]
Cs^{135}	134.948 67±10	Pr^{146}	145.963 58±12
Cs^{136}	135.950 65±9	Sm^{146}	145.959 29±6
Xe^{137}	136.954 6 ±11[c]	Nd^{147}	146.962 42±3
Cs^{137}	136.950 33±6	Pm^{147}	146.961 44±3
Cs^{138}	137.953 93±10	Pm^{148}	147.964 4 ±4[c]
Pr^{138}	137.953 9 ±3	Nd^{149}	148.967 37±16[b]
Ba^{139}	138.952 71±5[b]	Pm^{149}	148.965 59±20[c]
Ce^{139}	138.950 49±25	Pm^{150}	149.970 27±20
Pr^{139}	138.952 59±25[c]	Sm^{151}	150.967 64±13
Nd^{139}	138.957 0 ±3[c]	Eu^{152}	151.969 54±16
La^{140}	139.953 79±6[b]	Sm^{153}	152.970 1 ±4
Pr^{140}	139.953 28±6[b]	Sm^{155}	154.973 8 ±4
La^{141}	140.955 52±4	Eu^{155}	154.971 4 ±4
Ce^{141}	140.952 90±3[b]		

[a] Derived from Xe^{130} mass.
[b] Weighted average of two or more independent atomic masses.
[c] Doubtful reaction or β-decay data.
[d] Unweighted average of two or more independent atomic masses.

TABLE IV. New and corrected mass differences derived from reaction and β-decay data.

Mass difference	ΔM mMU	Reference
$Cs^{132} - Xe^{132}$	1.9 ±0.4	a
$Cs^{136} - Ba^{136}$	3.066±0.006	b
$Ba^{139} - Ba^{138} - 1$	3.919±0.011	c
$Ba^{139} - La^{139}$	2.556±0.025	d
$Ce^{141} - Pr^{141}$	0.621±0.002	e
$Pr^{142} - Nd^{142}$	2.319±0.013	f
$Ce^{143} - Pr^{143}$	1.550±0.004	g
$Nd^{144} - Ce^{140} - 4$	5.92 ±0.07	h
$Sm^{146} - Nd^{142} - 4$	6.69 ±0.05	i
$Sm^{147} - Nd^{143} - 4$	6.27 ±0.02	j
$Pm^{150} - Sm^{150}$	5.7 ±0.2	k
$Eu^{152} - Sm^{152}$	1.87 ±0.11	l

[a] B. L. Robinson and R. W. Fink, Phys. Rev. **98**, 231(A) (1955); A. H. Wapstra (unpublished): see A. H. Wapstra, Physica **21**, 385 (1955).
[b] J. L. Olsen and G. D. O'Kelley, Phys. Rev. **95**, 1539 (1954).
[c] Paris, Buechner, and Endt, Phys. Rev. **100**, 1317 (1955).
[d] A. C. G. Mitchell and E. Hebb, Phys. Rev. **95**, 727 (1954), estimated error.
[e] This is a weighted average of the data given by R. W. King, Revs. Modern Phys. **26**, 327 (1954) and J. T. Jones and E. N. Jensen, Phys. Rev. **97**, 1031 (1955).
[f] This is a weighted average of the data given by King (footnote e) and Pohm, Lewis, Talboy, and Jensen, Phys. Rev. **95**, 1523 (1954).
[g] Martin, Cork, and Burson, Phys. Rev. **99**, 670(A) (1955).
[h] Weighted average of data from Waldron, Schultz, and Kohman, Phys. Rev. **93**, 254 (1954) and W. Porschen and W. Riezler, Z. Naturforsch **9a**, 701 (1954).
[i] D. C. Dunlavey and G. T. Seaborg, Phys. Rev. **92**, 206 (1953).
[j] W. P. Jesse and J. Sadauskis, Phys. Rev. **78**, 1 (1950).
[k] V. K. Fischer, Phys. Rev. **96**, 1549 (1954).
[l] H. Kendall and L. Grodzins, Bull. Am. Phys. Soc. Ser. II, **1**, 164 (1956).

[9] Scolman, Quisenberry, and Nier, Phys. Rev. **102**, 1076 (1956).
[10] D. M. Van Patter and W. Whaling, Revs. Modern Phys. **26**, 402 (1954).
[11] R. W. King, Revs. Modern Phys. **26**, 327 (1954).
[12] Cohen, DuMond, Layton, and Rollett, Revs. Modern Phys. **27**, 363 (1955).

mass units," are compared in Table V with similar differences computed from the previously listed doublet data. In all cases, the two independent measurements agree within the quoted error. The excellent agreement between the two methods of measurement allows one to extend the technique of isotopic mass units to the direct determination of atomic masses. This technique is of particular value for cases in which hydrocarbon doublet measurements are impossible. The present masses of Sm^{148} and Sm^{149} were determined in this manner, the calculation being based on the masses of Sm^{147} and Sm^{150} derived from hydrocarbon doublet data.

Mass differences, determined from the stable atomic masses, may be compared with mass differences determined from Q values and total β-decay energies. The comparisons that can be made are listed in Table VI. The disagreement in the $Ba^{130}-Xe^{130}$ difference is probably due to an error in the Ba^{130} mass. The doublet used to determine the Ba^{130} mass was particularly difficult to measure. The cause of the disagreement found for the $Nd^{143}-Ce^{142}$ mass difference is difficult to determine from the mass data. Other mass differences in this region, included several in one of the paths of the $Nd^{143}-Ce^{142}$ reaction mass difference, are in agreement.

TABLE V. Isotopic mass units compared with the mass difference determined from doublet data.

Doublet	Isotopic mass difference amu	Mass difference from doublets amu
$Xe^{131}-Xe^{130}$	1.00187	1.00189±5
$Xe^{132}-Xe^{131}$	0.99942	0.99940±7
$Cs^{133}-Xe^{132}$	1.00132	1.00128±9
$Xe^{134}-Cs^{133}$	1.00053	1.00060±8
$Ba^{135}-Ba^{134}$	1.00154	1.00162±13
$Ba^{136}-Ba^{135}$	0.99919	0.99913±13
$Ba^{137}-Ba^{136}$	1.00157	1.00148±10
$Ba^{138}-Ba^{137}$	0.99975	0.99968±10
$Nd^{143}-Nd^{142}$	1.00243	1.00242±10
$Nd^{144}-Nd^{143}$	1.00056	1.00054±12
$Nd^{145}-Nd^{144}$	1.00278	1.00258±20
$Nd^{146}-Nd^{145}$	1.00082	1.00095±20
$Sm^{148}-Sm^{147}$	1.00025	
$Sm^{149}-Sm^{148}$	1.00271	
$Sm^{150}-Sm^{149}$	1.00042	
$Sm^{150}-Sm^{147}$	3.00338[a]	3.00337±7

[a] A sum of the results of the previous three "isotopic mass units."

DISCUSSION OF RESULTS

Several features of nuclear structure in the region about the 82-neutron shell closure may be investigated by employing the mass values listed in Tables II and III. Of particular interest is the influence of the shell closure on the binding energy of the last nucleon. The mass data are also useful in the study of several alpha and β decays.

Nucleon Binding Energies

When atomic mass data are employed to calculate binding energies, one must recognize that the calculated binding energy is the total binding energy of the atom, the sum of the nuclear and the electronic binding. For quantities calculated in the following paragraphs, the electronic binding energy contribution is quite small and has been neglected. Numerical values for the nucleon binding energies to be discussed in this section are listed in Table VII.

Information concerning the general characteristics of nuclear binding may be obtained from a study of the average binding energy per nucleon. A graphical representation of the average binding energy per nucleon of the stable nuclei from $A=102$ to $A=155$, as a function of A, is indicated in Fig. 3. Experimental errors are too small to be indicated. Even-A isotopes of each element are connected by a solid curve while the odd-A nuclei of all the elements in this region are connected by a dotted line. In general, the line connecting the even-A points is a smooth curve approximating a parabola.[5] Except for the isotopes of cerium, this behavior is evident in the present data. The average binding energy per nucleon of Ce^{142} is significantly lower than the curve passing through the three lighter cerium isotopes. Cerium is the only element that has stable isotopes

TABLE VI. A comparison of mass differences determined mass spectroscopically with mass differences derived from nuclear reaction and β-decay energies. In cases where different nuclear reactions can be used, these are specified in Column 1.

Mass difference	Mass difference in mMU Present	Nuclear	Δ[a]
$Ba^{130}-Xe^{130}$	3.30±0.20	2.73±0.02	0.57±0.20
$Cs^{133}-Xe^{132}-1$	1.28±0.13	1.20±0.48	0.08±0.50
$Ba^{134}-Cs^{133}$	999.44±0.10	999.56±0.11	−0.12±0.15
$La^{139}-Ba^{138}-1$	1.46±0.10	1.36±0.03	0.10±0.10
$La^{139}-La^{138}$	999.61±0.20	999.54±0.20	0.07±0.30
$Ce^{140}-La^{139}$	999.56±0.09	999.46±0.12	0.10±0.15
$Ce^{142}-Ce^{140}-2$	4.65±0.09	4.50±0.25	0.15±0.30
$Pr^{141}-Ce^{140}-1$ $Pr^{140}(\beta)$	2.52±0.07	2.34±0.13	0.18±0.15
$Pr^{141}-Ce^{140}-1$ $Ce^{141}(\beta)$	2.52±0.07	2.58±0.11	−0.06±0.13
$Ce^{142}-Pr^{141}-1$	2.13±0.07	1.93±0.20	0.20±0.21
$Nd^{142}-Pr^{141}-1$ $Pr^{141}(d,p)Pr^{142}$	0.32±0.04	0.63±0.20	−0.31±0.20
$Nd^{142}-Pr^{141}-1$ $Pr^{141}(n,\gamma)Pr^{142}$	0.32±0.04	≦0.42±0.03	
$Nd^{143}-Nd^{142}-1$	2.42±0.10	2.53±0.08	−0.11±0.13
$Nd^{143}-Ce^{142}-1$ $Ce^{143}(\beta)$	0.61±0.12	0.98±0.07	−0.37±0.14
$Nd^{143}-Ce^{142}-1$ $Pr^{141}(d,p)Pr^{142}$	0.61±0.12	1.2 ±0.3	0.6 ±0.3
$Nd^{143}-Ce^{142}-1$ $Pr^{141}(n,\gamma)Pr^{142}$	0.61±0.12	≦1.02	
$Nd^{144}-Ce^{140}-4$	5.81±0.09	5.92±0.07	−0.11±0.11
$Sm^{147}-Nd^{143}-4$	6.18±0.11	6.27±0.02	−0.09±0.11
$Nd^{150}-Sm^{149}-1$	4.34±0.20	4.18±0.25	0.16±0.30
$Sm^{150}-Sm^{149}-1$ $Sm^{149}(n,\gamma)Sm^{150}$[b]	0.42±0.20	2.4 ±0.3	2.0 ±0.4
$Sm^{150}-Sm^{149}-1$ $Sm^{149}(n,\gamma)Sm^{150}$[c]	0.42±0.20	≦0.51±0.06	

[a] Present mass difference minus nuclear mass difference in mMU.
[b] See reference 25.
[c] See reference 16.

TABLE VII. The average binding energy per nucleon, B.E./A, the binding energy of the last neutron B_n, the binding energy of the last pair of neutrons B_{2n}, and the binding energy of the last proton B_p for all nuclei for which there are sufficient data to calculate these values. All values listed in mMU.

Isotope	B.E./A[a]	B_n	B_{2n}	B_p
$_{54}Xe_{76}^{130}$	9.060			
Xe_{77}^{131}	9.045	7.09±0.05		
Xe_{78}^{132}	9.049	9.58±0.07	16.68±0.06	
Xe_{79}^{133}	9.036	7.24±0.09		
Xe_{80}^{134}	9.034	8.85±0.08	16.09±0.07	
Xe_{81}^{135}	9.020	7.04±0.11		
Xe_{82}^{136}	9.016	8.50±0.10	15.54±0.05	
Xe_{83}^{137}	8.985±0.008	4.8 ±1.1		
$_{55}Cs_{75}^{130}$	9.029			
Cs_{76}^{131}	9.036	9.95±0.05		5.89±0.05
Cs_{77}^{132}	9.028	7.95±0.20		6.74±0.20
Cs_{78}^{133}	9.033	9.70±0.20	17.65±0.08	6.86±0.09
Cs_{79}^{134}	9.020	7.31±0.09		6.93±0.09
Cs_{80}^{135}	9.023	9.38±0.12	16.68±0.12	7.46±0.14
Cs_{81}^{136}	9.008	7.01±0.13		7.43±0.13
Cs_{82}^{137}	9.010	9.31±0.10	16.32±0.11	8.24±0.06
Cs_{83}^{138}	8.984	5.38±0.11		8.8 ±1.1
$_{56}Ba_{74}^{130}$	9.022			
Ba_{76}^{132}	9.029		19.01±0.25	8.15±0.13
Ba_{78}^{134}	9.030		18.20±0.14	8.70±0.10
Ba_{79}^{135}	9.018	7.36±0.13		8.76±0.12
Ba_{80}^{136}	9.024	9.86±0.13	17.22±0.12	9.24±0.13
Ba_{81}^{137}	9.013	7.51±0.10		9.73±0.11
Ba_{82}^{138}	9.015	9.31±0.10	16.82±0.12	9.74±0.10
Ba_{83}^{139}	8.987	5.01±0.09		9.37±0.10
$_{57}La_{77}^{134}$	8.994±0.002			
La_{81}^{138}	8.996			6.61±0.21
La_{82}^{139}	8.999	9.38±0.20		6.68±0.10
La_{83}^{140}	8.973	5.39±0.09		7.06±0.8
La_{84}^{141}	8.961	7.26±0.07	12.65±0.07	
$_{58}Ce_{78}^{136}$	8.992			
Ce_{80}^{138}	8.995		18.4 ±0.3	
Ce_{81}^{139}	8.990±0.002	8.36±0.30		8.2 ±0.3
Ce_{82}^{140}	8.996	9.72±0.25	18.08±0.20	8.59±0.09
Ce_{83}^{141}	8.973	5.84±0.07		9.03±0.07
Ce_{84}^{142}	8.963	7.48±0.07	13.32±0.09	9.25±0.08
Ce_{85}^{143}	8.940	5.67±0.16		
Ce_{86}^{144}	8.931	7.63±0.16	13.30±0.25	
Ce_{88}^{146}	8.893		12.36±0.17	
$_{59}Pr_{79}^{138}$	8.960±0.002			
Pr_{80}^{139}	8.969±0.002	10.3 ±0.4		5.4 ±0.3
Pr_{81}^{140}	8.964	8.29±0.25		5.35±0.25
Pr_{82}^{141}	8.972	9.99±0.06	18.28±0.25	5.62±0.07
Pr_{83}^{142}	8.953	6.31±0.04		6.09±0.04
Pr_{84}^{143}	8.946	7.92±0.10	14.23±0.10	6.54±0.12
Pr_{85}^{144}	8.927	6.25±0.12		7.12±0.08
Pr_{87}^{146}	8.895			
$_{60}Nd_{79}^{139}$	8.932±0.002			5.0 ±0.4
Nd_{81}^{141}	8.953			7.35±0.12
Nd_{82}^{142}	8.964	10.47±0.11		7.83±0.04
Nd_{83}^{143}	8.947	6.56±0.10		8.08±0.10
Nd_{84}^{144}	8.943	8.44±0.12	15.00±0.07	8.69±0.09
Nd_{85}^{145}	8.926	6.41±0.20		8.77±0.20
Nd_{86}^{146}	8.920	8.04±0.20	14.45±0.09	
Nd_{87}^{147}	8.897	5.65±0.07		9.31±0.12
Nd_{88}^{148}	8.891	7.92±0.07	13.56±0.08	
Nd_{89}^{149}	8.865	5.10±0.17		
Nd_{90}^{150}	8.859	7.87±0.17	12.97±0.09	
$_{61}Pm_{86}^{147}$	8.898			5.79±0.07
Pm_{87}^{148}	8.879±0.003	6.1 ±0.4		6.2 ±0.4
Pm_{88}^{149}	8.872	7.7 ±0.4	13.82±0.20	6.04±0.20
Pm_{89}^{150}	8.841	4.3 ±0.3		5.25±0.25
$_{62}Sm_{82}^{144}$	8.919			
Sm_{84}^{146}	8.905		16.10±0.11	
Sm_{85}^{147}	8.894	7.07±0.07		
Sm_{86}^{148}	8.893	8.73±0.20	15.80±0.20	8.14±0.20
Sm_{87}^{149}	8.876	6.3 ±0.3		8.3 ±0.4
Sm_{88}^{150}	8.874	8.57±0.20	14.85±0.20	9.17±0.20
Sm_{89}^{151}	8.854	5.91±0.15		10.77±0.25
Sm_{90}^{152}	8.855	8.96±0.18	14.87±0.15	
Sm_{91}^{153}	8.840±0.002	6.6 ±0.4		
Sm_{92}^{154}	8.836	8.2 ±0.4	14.77±0.20	
Sm_{93}^{155}	8.817±0.002	6.0 ±0.4		
$_{63}Eu_{88}^{151}$	8.849			5.18±0.15
Eu_{89}^{152}	8.837	6.98±0.20		6.24±0.20
Eu_{90}^{153}	8.840±0.002	9.3 ±0.4	16.0 ±0.4	6.6 ±0.4
Eu_{92}^{155}	8.827±0.002		16.3 ±0.5	7.6 ±0.4

[a] Errors for this column are ±0.001 mMU unless otherwise indicated.

both above and below the shell closure at $N=82$. This departure from uniformity for the average binding energy per nucleon results is undoubtedly due to the influence of the shell closure. The change in slope of the odd-A line that occurs at about $A=139$ is also undoubtedly associated with the shell closure. Earlier, less complete data by Hogg and Duckworth[14] also showed this change in slope.

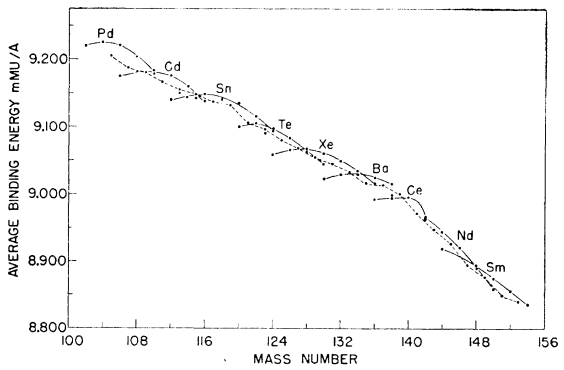

FIG. 3. Average binding energy per nucleon. Results for $A<130$ were derived from mass measurements by Halsted; see reference 4.

A more revealing study of the effect of shell closures on the binding energy systematics of nuclei may be made by investigation of the behavior of the binding energy of the last nucleon in the region near the shell closure. Binding energies of the last neutron B_n in this region are known from (γ,n) thresholds[15] and (n,γ)[16] and (d,p) reactions.[17] Investigations by β-energy systematics yield the change in neutron binding energy as the shell is traversed. All methods of measurement indicate that there is a discontinuity in B_n of approximately 2 mMU as the shell is crossed.

By combining reaction and β-decay data with the stable atomic mass data, the discontinuity in B_n can be investigated in considerably greater detail than has

[14] B. G. Hogg and H. E. Duckworth, Can. J. Phys. **32**, 65 (1954).
[15] Sher, Halpern, and Mann, Phys. Rev. **84**, 387 (1951).
[16] B. B. Kinsey and G. A. Bartholomew, Can. J. Phys. **31**, 1051 (1953).
[17] N. S. Wall, Phys. Rev. **96**, 664 (1954).

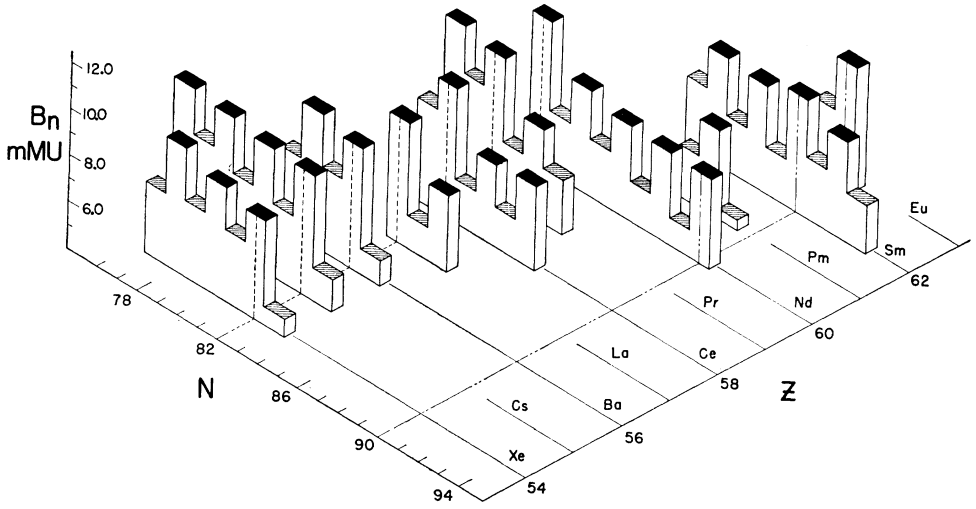

FIG. 4. An isometric view of the binding energy of the last neutron B_n plotted as a function of Z and N.

previously been possible. The masses listed in Table II and Table III are employed to calculate 58 values for B_n in the region $A=130$ to 155. These neutron binding energies are plotted in Fig. 4. It is apparent that the discontinuity in binding energy is caused by a decrease in neutron binding energy for neutrons beyond $N=82$ rather than a particularly high binding energy at neutron 82. This decrease in B_n is particularly noticeable for the elements cerium and praseodymium for which several binding energies, both above and below the shell closure, are available. In order to compare the change in B_n determined from the present data with that obtained in previous investigations, one must compare the difference in binding between neighboring paired or unpaired neutrons; that is, $N=81$ to $N=83$ or $N=82$ to $N=84$. The present results yield an average decrease in B_n of 2.15 mMU, a value in good agreement with previous results. This result, however, is not completely independent of the previous results because much of the experimental data employed previously is included in the present study.

A somewhat simplified study of the variation in binding energy may be made by considering the binding energy of the last pair of neutrons B_{2n} in an even-neutron-number nucleus. These data, plotted in Fig. 5 as a function of the neutron number N, rely more on stable masses and thus are less likely to change if mass differences, derived from reaction and β-decay data, are modified. There is an approximately linear decrease in B_{2n} as the neutron number is increased. For a given neutron number, the B_{2n} values increase as Z increases. The discontinuity in binding energy, caused by the shell closure, is again apparent in the data for cerium and praseodymium. There is a tendency for B_{2n} at neutron numbers 78, 82, 86, and 90 to be somewhat larger than might be expected from a linear extrapolation through the remaining data. One finds that these somewhat larger B_{2n} values correspond to an even number of pairs of neutrons in a given shell. Although these variations are about equal in magnitude to the quoted errors, it seems quite likely that the effect is real because it appears so consistently.

With the present table of masses, it is possible to calculate the binding energy of the last proton B_p for 47 nuclei in this region. With these data, shown in Fig. 6, a study of the effect of the neutron shell closure on the proton binding may be made. Generally, the B_p values for a particular element increase as the neutron number increases. Also, even-Z elements have larger B_p values than neighboring odd-Z elements. In the group of nuclei which display the discontinuity in B_n, Ba^{139} is the only nucleus which does not obey the general trend of proton binding. Thus, the discontinuity in the atomic masses at the shell closure is directly due to the change in neutron binding.

Nucleon Pairing Energies

One can observe that the nucleon binding energy for protons or neutrons is greater for even Z or N, respectively, than for odd Z or N. The pairing effect is the cause of this behavior. For every pair of like nucleons that are added to form a nucleus, the total binding

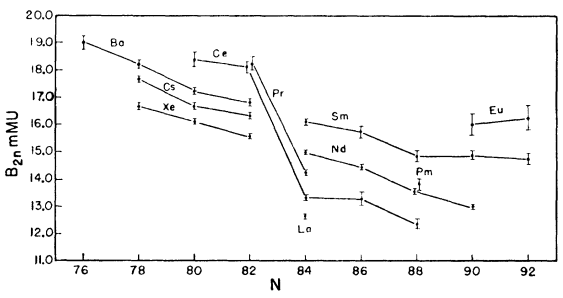

FIG. 5. The binding energy of the last pair of neutrons B_{2n} in the nucleus.

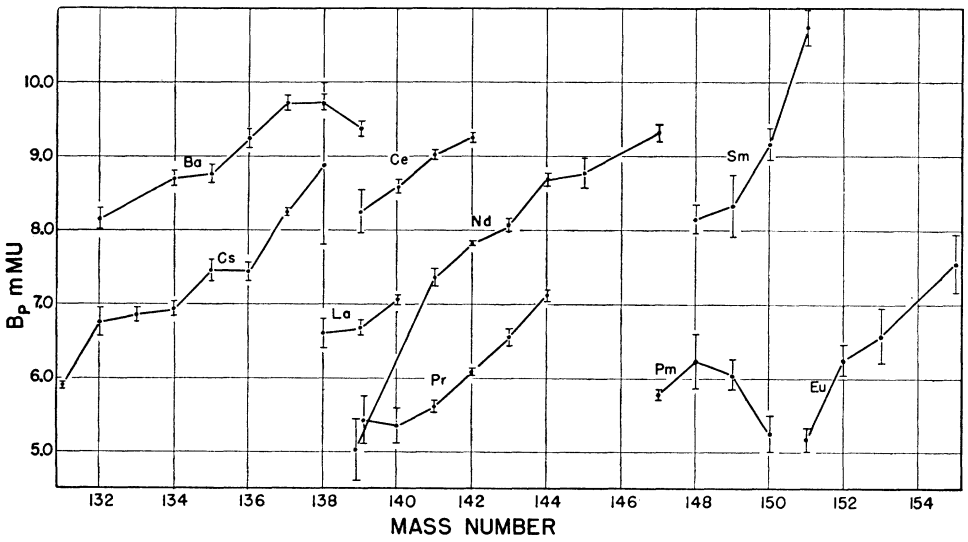

FIG. 6. The binding energy of the last proton B_p in the nucleus.

energy of the nucleus is increased by an amount P above the simple sum of the individual binding energies of each nucleon added. The excess binding energy P, called the pairing energy, can be calculated easily from the nucleon binding energy data. As an example, the neutron pairing energy P_n of the last pair of neutrons in the nucleus (Z,N) is

$$P_n(Z,N)=B_n(Z,N)-B_n(Z,N-1), \quad N \text{ even}. \quad (1)$$

It has been observed, in the light nuclei, that pairing energy increases as the total angular momentum quantum number of the level containing the pair increases.[18] Measurements of nuclear spin indicate that the $2d_{\frac{3}{2}}$ (shell model) energy level is filled to reach the 82-neutron shell closure, and that following the shell closure, the $2f_{7/2}$ level is filled. Thus one might expect an increase in neutron pairing energy beyond the 82 neutron shell closure. Experimental pairing energies listed in Table VIII and shown graphically as a function of neutron number N in Fig. 7 do not indicate this predicted increase. The quoted errors are rather large and also, because three different masses are employed in the calculation, the possibility of undiscovered experimental errors is increased. For these reasons, few generalizations should be developed from these data.

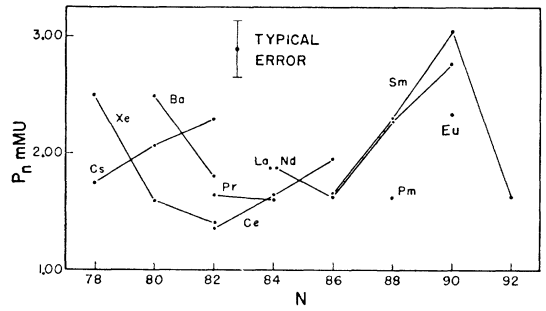

FIG. 7. The pairing energy of the last pair of neutrons P_n in the nucleus.

Proton pairing energies P_p can be calculated for the even-Z elements. To obtain P_p from atomic mass data one must consider the small change in the Coulomb energy of the three nuclei involved in the calculation. In this region the Coulomb correction is small and essentially constant, and therefore has been neglected in these calculations. The proton pairing energies that can be calculated from the mass data are found in Table IX and plotted as a function of the neutron number N in Fig. 8. For reasons similar to those given in the preceding paragraph, few generalizations should be made from these data.

Typical neutron and proton pairing energies in this region are of the order of 2 mMU. A similar average value for pairing energies has been found by Quisenberry *et al.*[5] for the region near $A=60$. This average pairing energy is somewhat smaller than that found for the light nuclei.

90 Neutron Binding Energy Anomaly

A change in the nuclear structure in the neighborhood of 90 neutrons has been indicated by anomalies in the isotope shift,[19] quadrupole moments,[20] and Coulomb excitation energy levels.[21] In particular, a very large isotope shift, an increase in the quadrupole moment, and a sharp decrease in the rotational state energies has been observed between 88 and 90 neutrons.

Mottelson and Nilsson[22] employ an ellipsoidal po-

[18] M. G. Mayer and J. H. D. Jensen, *Elementary Theory of Nuclear Shell Structure* (John Wiley and Sons, Inc., New York, 1955).

[19] P. Brix and H. Kopfermann, Phys. Rev. **85**, 1050 (1952).
[20] P. Brix, Z. Physik **132**, 579 (1952).
[21] N. P. Heydenberg and G. M. Temmer, Phys. Rev. **100**, 150 (1955).
[22] B. R. Mottelson and S. G. Nilsson, Phys. Rev. **99**, 1615 (1955).

tential with a spin-orbit force to calculate the individual-particle energy levels as a function of nuclear distortion. With this spectrum, the ground state equilibrium deformations are calculated for nuclei in the region $N=82$ to $N=126$. A sharp increase in nuclear deformation is predicted in going from 88 to 90 neutrons, in agreement with the trend of deformation deduced from experimental data.

Several abnormalities exist in the binding-energy data in the neighborhood of 90 neutrons. In Fig. 4, neutron binding energies for samarium nuclei from $N=85$ to $N=93$ are shown. There is a rather obvious increase in B_n at $N=90$ (Sm^{152}). Although the quoted errors for B_n are rather large, there is little doubt that the increase exists. The $N=90$ isotope of neodymium has a somewhat higher neutron binding compared with the systematics of the other even-N neodymium binding energies, but the increase is not as pronounced as that found for samarium.

Figure 7 indicates a sharp increase in the neutron pairing energy following $N=86$, with the maximum at

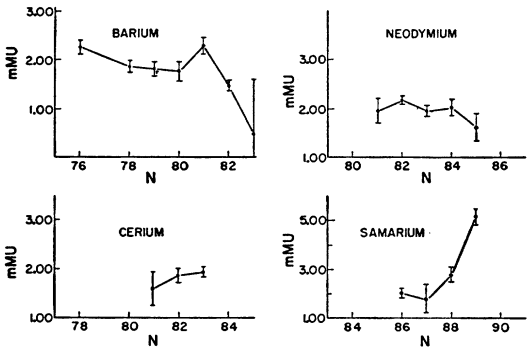

FIG. 8. The pairing energy of the last pair of protons P_p in the nucleus.

$N=90$. For isotopes of samarium and neodymium having equal neutron numbers, the neutron pairing energies for $N=86$, 88, and 90 appear to be the same within the experimental errors. The neutron pairing energy of Sm^{154} ($N=92$) again falls to a value equal to that at $N=86$. The P_n value for europium at $N=90$ is also abnormally large.

Proton binding and pairing energies also show a somewhat anomalous behavior in nuclei having neutron numbers near 90. Because of possible misinterpretation in the β-decay energy data for several promethium isotopes, these data are less reliable than the neutron data. Proton pairing energies for the nuclei of samarium having $N=88$ and $N=89$ are abnormally large; see Fig. 8. Unfortunately, there are insufficient data to calculate proton pairing energies for nuclei with N greater than 89.

Reaction Assignments

The neutron binding energy results can be employed to make isotopic assignments for several previously unassigned (n,γ) and (γ,n) reactions. Sher, Halpern, and Mann[15] measured gamma-ray thresholds for the (γ,n) reaction for barium, finding thresholds of 6.80 $\pm$0.20 and 8.55$\pm$0.25 Mev. The 8.55-Mev neutron binding energy is in agreement with the B_n value for Ba^{138} (8.67$\pm$0.10 Mev). Thus, the target nucleus is Ba^{138}. No unique prediction of target nucleus can be made for the other reaction. The threshold measurement (6.80$\pm$0.20 Mev) is not accurate enough to distinguish between the B_n values found for Ba^{135} (6.85$\pm$0.12 Mev) and Ba^{137} (6.99$\pm$0.10 Mev).

Kinsey and Bartholomew[16] have reported eleven de-excitation gamma rays from the thermal-neutron capture reaction on barium. The gamma rays having energies 4.70$\pm$0.03 and 4.10$\pm$0.03 Mev have been assigned to the reaction $Ba^{138}(n,\gamma)Ba^{139}$ by Paris *et al.*[23] Kinsey and Bartholomew tentatively assigned the gamma ray with the highest energy (9.23$\pm$0.07 Mev) to the reaction $Ba^{137}(n,\gamma)Ba^{138}$. The mass data indicate that this gamma ray should be assigned to the reaction $Ba^{135}(n,\gamma)Ba^{136}$ having a Q-value 9.18$\pm$0.12 Mev found from mass data. The gamma rays with energies 7.18 $\pm$0.06 and 6.68$\pm$0.06 Mev should probably be assigned

TABLE VIII. Pairing energy of the last pair of neutrons in the listed isotope.

Isotope	Neutron number	P_n in mMU	Isotope	Neutron number	P_n in mMU
Xe^{132}	78	2.49±0.09	Pr^{141}	82	1.7 ±0.3
Xe^{134}	80	1.60±0.12	Pr^{143}	84	1.61±0.11
Xe^{136}	82	1.41±0.15			
			Nd^{144}	84	1.87±0.16
Cs^{133}	78	1.8 ±0.3	Nd^{146}	86	1.6 ±0.3
Cs^{135}	80	2.07±0.15	Nd^{148}	88	2.27±0.09
Cs^{137}	82	2.29±0.16	Nd^{150}	90	2.77±0.25
Ba^{136}	80	2.49±0.18	Pm^{149}	88	1.7 ±0.6
Ba^{138}	82	1.80±0.14			
			Sm^{148}	86	1.65±0.20
La^{141}	84	1.87±0.12	Sm^{150}	88	2.3 ±0.4
			Sm^{152}	90	3.04±0.25
Ce^{140}	82	1.4 ±0.4	Sm^{154}	92	1.7 ±0.6
Ce^{142}	84	1.64±0.10			
Ce^{144}	86	1.95±0.20	Eu^{153}	90	2.3 ±0.5

TABLE IX. Pairing energy of the last pair of protons in the listed isotope.

Isotope	Neutron number	P_p in mMU	Isotope	Neutron number	P_p in mMU
Ba^{132}	76	2.27±0.14	Nd^{141}	81	2.00±0.25
Ba^{134}	78	1.87±0.13	Nd^{142}	82	2.21±0.08
Ba^{135}	79	1.83±0.15	Nd^{143}	83	1.99±0.11
Ba^{136}	80	1.78±0.19	Nd^{144}	84	2.06±0.17
Ba^{137}	81	2.30±0.17	Nd^{145}	85	1.65±0.25
Ba^{138}	82	1.49±0.11			
Ba^{139}	83	0.5 ±1.1	Sm^{148}	86	2.35±0.20
			Sm^{149}	87	2.1 ±0.6
Ce^{139}	81	1.6 ±0.4	Sm^{150}	88	3.1 ±0.3
Ce^{140}	82	1.91±0.13	Sm^{151}	89	5.5 ±0.4
Ce^{141}	83	1.97±0.11			

[23] Paris, Buechner, and Endt, Phys. Rev. **100**, 1317 (1955).

to the reactions $Ba^{136}(n,\gamma)Ba^{137}$ (6.99±0.10 Mev) and $Ba^{134}(n,\gamma)Ba^{135}$ (6.85±0.12 Mev), respectively. A level with an excitation energy of 2.88 Mev[24] has been reported in Ba^{138}. Good agreement with the mass data is obtained if the 5.74±0.03 Mev gamma ray found by Kinsey and Bartholomew is assigned to the Ba^{138} nucleus. This gamma ray must then feed the 2.88-Mev level. The total de-excitation energy of 8.62 Mev agrees well with the value of 8.67±0.10 Mev, derived from the mass data. Therefore this gamma ray is assigned to the $Ba^{137}(n,\gamma)Ba^{138}$ reaction.

Kinsey and Bartholomew[16] have investigated the $Sm^{149}(n,\gamma)Sm^{150}$ reaction and find the neutron binding energy in Sm^{150} to be at least 7.89±0.06 Mev. Kubitschek and Dancoff,[25] investigating the same reaction, find the neutron binding energy to be 6.6±0.03 Mev. The mass data, yielding a B_n value of 7.98±0.20 Mev, are consistent with the measurement of Kinsey and Bartholomew, and are also in agreement with the results of Adyasevich *et al.*[26] who infer the B_n value of Sm^{150} to be 8.00±0.03 Mev. The possibility exists that Kubitschek and Dancoff measured the gamma ray from the reaction $Sm^{152}(n,\gamma)Sm^{153}$. The mass data predict a gamma-ray energy of 6.1±0.4 Mev for this reaction.

Radioactive Decay Energies

Several radioactive nuclei in the rare earth region have sufficiently long half-lives so their natural abundance is large enough to permit a mass spectroscopic determination of their masses. The mass data then can be employed to study the decay schemes of these nuclei.

Natural alpha activity has been observed for samarium[27] and neodymium,[28,29] with the activity assigned to Sm^{147} and Nd^{144}, respectively. The mass differences, derived from the present mass measurements, predict alpha energies which agree with those observed directly. Although the mass data show that most of the naturally occurring neodymium and samarium isotopes have sufficient energy to be alpha active, the largest possible decay energy in each of these elements occurs in the isotope to which the activity is assigned. It is possible to infer from the mass data that an alpha decay from Ce^{142} to Ba^{138} might be experimentally observable. The total available energy for this decay is 1.68±0.10 Mev.

The masses of the triple isobar at mass 138 were determined. The available energy calculated from the mass data for the decay of La^{138} to Ba^{138} is 1.73±0.20 Mev and for the decay of La^{138} to Ce^{138} is 0.7±0.3 Mev. Truchinetz and Pringle[30] found a 0.81-Mev and a 1.43-Mev gamma ray following the decay of La^{138}. They show that the 1.43-Mev gamma ray is in coincidence with a barium x-ray while the 0.81-Mev gamma ray is not. The 1.43-Mev gamma ray is therefore assigned to the K capture to Ba^{138} and the 0.81 Mev is assigned to a de-excitation of the Ce^{138} nucleus following β decay. From a measurement of the L/K capture ratio they conclude that the total available decay energy of La^{138} to Ba^{138} is 1.59±0.04 Mev. Beta systematics were employed to predict the β-decay energy to the 0.81-Mev level to be 5 to 10 kev. Glover and Watt[31] report a β decay with an end point at 0.205 Mev, presumably followed by the 0.81 Mev de-excitation gamma ray in Ce^{138}. Thus, the total energy available for the decay to Ce^{138} is at least 0.81 Mev and probably 1.01 Mev. Either of these values is in agreement with the measurements of Mulholland and Kohman[32] who find a maximum β-decay energy of 1.0±0.2 Mev.

The mass results agree in general with the decay scheme proposed for La^{138}. However, the agreement of the available energy for the decay to Ba^{138} from the mass results (1.73±0.20 Mev) with the available energy derived from a chain of reactions (1.71±0.19 Mev) suggests that the available decay energy for the La^{138} to Ba^{138} decay that was estimated by Truchinetz and Pringle might be somewhat low.

Doubt whether Nd^{150} is stable toward single β decay has existed for some time. Kohman[33] has shown by means of a semiempirical mass formula that Nd^{150} is beyond the limit of beta stability. The measurement of the $Nd^{150}-Sm^{150}$ mass difference by Hogg and Duckworth[14] together with the $Pm^{150}-Sm^{150}$ mass difference 5.30±0.15 Mev determined by Fischer[34] can be employed to show that the $Nd^{150}-Pm^{150}$ mass difference is −0.7±1.0 Mev. Hogg[35] has employed β-energy systematics to conclude that the $Nd^{150}-Sm^{150}$ mass difference measured by Hogg and Duckworth may be too large by about 0.6 Mev. If account is taken of this, the $Nd^{150}-Pm^{150}$ mass difference becomes −1.3±1.0 Mev and Nd^{150} would be stable toward single β decay. The conclusion by Hogg can be experimentally verified with the present doublet data. Our $Nd^{150}-Sm^{150}$ mass difference of 3.65±0.10 Mev is somewhat lower than the mass difference assumed by Hogg, 4.0±0.8 Mev. When our mass difference is combined with the $Pm^{150}-Sm^{150}$ value of Fischer, a $Nd^{150}-Pm^{150}$ mass difference of −1.65±0.18 Mev is found. Thus Nd^{150} is stable toward single β decay.

[24] Langer, Duffield, and Stanley, Phys. Rev. **89**, 907(A) (1953).
[25] H. Kubitschek and S. M. Dancoff, Phys. Rev. **76**, 531 (1949).
[26] Adyasevich, Grosher, and Demidov, Conf. Acad. USSR on Peaceful Use of Atomic Energy, Phys. Math. Sc., p. 270, July (1955).
[27] W. P. Jesse and J. Sadauskis, Phys. Rev. **78**, 1 (1950).
[28] Waldron, Schultz, and Kohman, Phys. Rev. **93**, 254 (1954).
[29] W. Porschen and W. Riezler, Z. Naturforsch. **9A**, 701 (1954).
[30] W. Turchinetz and R. W. Pringle, Phys. Rev. **103**, 1000 (1956).
[31] R. N. Glover and D. E. Watt, Phil. Mag. (to be published). See note added in proof in reference 30.
[32] G. I. Mulholland and T. P. Kohman, Phys. Rev. **87**, 681 (1952).
[33] T. P. Kohman, Phys. Rev. **73**, 16 (1948).
[34] V. K. Fischer, Phys. Rev. **96**, 1549 (1954).
[35] B. G. Hogg, Phys. Rev. **99**, 175 (1955).

ACKNOWLEDGMENTS

The pure samples of rare earth metals were supplied by the Ames Laboratory of the U. S. Atomic Energy Commission through the courtesy of Dr. F. H. Spedding. The authors wish to acknowledge this assistance. The construction of the apparatus was aided materially by grants from the Graduate School and the Minnesota Technical Research Fund subscribed to by General Mills, Inc., *Minneapolis Star and Tribune*, Minnesota Mining and Manufacturing Company, Northern States Power Company, and Minneapolis Honeywell Regulator Company.

PHYSICAL REVIEW VOLUME 105, NUMBER 3 FEBRUARY 1, 1957

Energy Levels of Ca^{43}†

C. M. BRAAMS*
Physics Department and Laboratory for Nuclear Science, Massachusetts Institute of Technology, Cambridge, Massachusetts
(Received October 19, 1956)

The $Ca^{42}(d,p)Ca^{43}$ and $Ca^{43}(p,p')Ca^{43}$ reactions were investigated with the MIT-ONR electrostatic generator and a magnetic broad-range spectrograph. Bombarding energies from 5.0 to 7.4 Mev were used; targets were made of magnetically separated isotopes. The Q-value of the $Ca^{42}(d,p)Ca^{43}$ ground-state transition is 5.711 ± 0.010 Mev. Thirty excited states of Ca^{43} in the region below 3.43 Mev are well established.

I. INTRODUCTION

IN two previous papers,[1,2] which will be referred to as I and II, we have described experiments on the $Ca^{40}(p,p')Ca^{40}$ and $Ca^{40}(d,p)Ca^{41}$ reactions. The present paper deals with (d,p) and (p,p') reactions on targets enriched in Ca^{42} and Ca^{43}, respectively.

The β^- decay of K^{43} and the β^+ decay of Sc^{43} are complex and yield information about the low-lying levels of Ca^{43}. The results have been compiled by the Nuclear Data Project.[3] The most detailed measurements on the decay of K^{43} and Sc^{43} are those by Lindqvist and Mitchell,[4,5] but work by Nussbaum *et al.*[6] and by van Lieshout and Hayward[7] disagrees with that by Lindqvist and Mitchell on several points. A level at 0.374 Mev is evident in the decay of Sc^{43}; and, from conflicting reports, Way *et al.*[3] have accepted a 1.05-Mev level, excited by electron capture in Sc^{43}. The two most prominent gamma rays accompanying the decay of K^{43} have energies of 0.369 and 0.627 Mev, as measured by Lindqvist and Mitchell. From β^--decay energies and relative intensities of gamma rays, these authors conclude that there is a cascade from 0.996 Mev via 0.627 Mev to the ground state. They also find levels at 1.389 and 1.608 Mev.

II. EXPERIMENTAL RESULTS

Our experimental techniques were similar to those described in other publications from this Laboratory (see I and II and references given there). The present work was done chiefly with the new broad-range spectrograph. Magnetically separated isotopes were used in the targets; the isotopes were supplied as $CaCO_3$ by the Oak Ridge National Laboratories. The material was heated in a tantalum boat. At 825°C, the carbonate decomposed into CaO and CO_2; and at about 2700°C, the oxide evaporated onto backings of thick platinum or thin Formvar reinforced with gold leaf. The abundances of the isotopes in the enriched samples are listed in Table I.

Surveys of the spectrum of protons from the $Ca^{42}(d,p)Ca^{43}$ reaction were taken with the 180-degree spectrograph with bombarding energies of 2.9 and 5.0 Mev. Because of the presence of Ca^{40} in the concentrated Ca^{42}, the proton groups from the excited states of Ca^{41} interfered with the Ca^{43} spectrum in the region of excitation of Ca^{43} above 1.5 Mev (see Fig. 1 of II). The groups from the ground state and four excited states of Ca^{43}, however, fell between the groups from the ground state and the first excited state of Ca^{41}, so that the ground-state Q-value and the excitation energies of these four levels could be measured.[8]

TABLE I. Abundances of calcium isotopes in natural and enriched samples.

Sample	Ca^{40}	Ca^{42}	Ca^{43}	Ca^{44}	Ca^{46}	Ca^{48}
Natural	96.96	0.64	0.145	2.06	0.003	0.185
Ca^{42}	35.44	64.17	0.06	0.32	0.001	0.01
Ca^{43}	23.38	1.64	67.95	7.03	<0.01	<0.01

† This work has been supported in part by the joint program of the Office of Naval Research and the U. S. Atomic Energy Commission.
* Present address: Physisch Laboratorium, Utrecht, Netherlands.
[1] C. M. Braams, Phys. Rev. **101**, 1764 (1956).
[2] C. M. Braams, Phys. Rev. **103**, 1310 (1956).
[3] *Nuclear Level Schemes*, compiled by Way, King, McGinnis, and van Lieshout, Atomic Energy Commission Report TID 5300 (U. S. Government Printing Office, Washington, D. C., 1955).
[4] T. Lindqvist and A. C. G. Mitchell, Phys. Rev. **95**, 444 (1954).
[5] T. Lindqvist and A. C. G. Mitchell, Phys. Rev. **95**, 1535 (1954).
[6] Nussbaum, van Lieshout, and Wapstra, Phys. Rev. **92**, 207 (1953) and R. H. Nussbaum, Ph.D. thesis, Amsterdam, 1954 (unpublished).
[7] R. van Lieshout and R. W. Hayward, quoted by K. Way *et al.*, reference 3.
[8] C. M. Braams, Phys. Rev. **95**, 650(A) (1954).